$\dot{V}/\dot{Q}$ distribution and correlation to atelectasis in anesthetized paralyzed humans

LEIF TOKICS, GÖRAN HEDENSTIERNA, LEIF SVENSSON, BO BRISMAR, TORSTEN CEDERLUND, HANS LUNDQUIST, AND ÅKE STRANDBERG
Departments of Anesthesiology, Hospital Physics, Surgery, and Roentgenology, Huddinge University Hospital, S-141 86 Huddinge; and Department of Clinical Physiology, University Hospital of Uppsala, S-751 85 Uppsala, Sweden

Tokics, Leif, Göran Hedenstierna, Leif Svensson, Bo Brismar, Torsten Cederlund, Hans Lundquist, and Åke Strandberg. $\dot{V}/\dot{Q}$ distribution and correlation to atelectasis in anesthetized paralyzed humans. *J. Appl. Physiol.* 81(4): 1822–1833, 1996.—Regional ventilation and perfusion were studied in 10 anesthetized paralyzed supine patients by single-photon emission computerized tomography. Atelectasis was estimated from two transaxial computerized tomography scans. The ventilation-perfusion ($\dot{V}/\dot{Q}$) distribution was also evaluated by multiple inert gas elimination. While the patients were awake, inert gas $\dot{V}/\dot{Q}$ ratio was normal, and shunt did not exceed 1% in any patient. Computerized tomography showed no atelectasis. During anesthesia, shunt ranged from 0.4 to 12.2%. Nine patients displayed atelectasis (0.6–7.2% of the intrathoracic area), and shunt correlated with the atelectasis ($r = 0.91$, $P < 0.001$). Shunt was located in dependent lung regions corresponding to the atelectatic area. There was considerable $\dot{V}/\dot{Q}$ mismatch, with ventilation mainly of ventral lung regions and perfusion of dorsal regions. Little perfusion was seen in the most ventral parts (zone 1) of caudal (diaphragmatic) lung regions. In summary, shunt during anesthesia is due to atelectasis in dependent lung regions. The $\dot{V}/\dot{Q}$ distributions differ from those shown earlier in awake subjects.

lung; ventilation-perfusion; ventilation; mechanical ventilation; computerized X-ray tomography; single-photon emission computerized tomography

DURING GENERAL ANESTHESIA, atelectasis develops promptly in dependent lung regions during spontaneous breathing and mechanical ventilation and whether the anesthetic is given intravenously or is inhaled (2, 8, 27, 30). The visualization of atelectasis requires computerized tomography (CT) of the lung; in most cases, conventional pulmonary X-ray does not disclose the densities. The atelectasis has been shown to be perfused by blood (28), and the size of atelectatic lung regions has been shown to correlate with the magnitude of shunt (8, 30). However, it has not been possible to locate shunt to any particular lung region.

In the present investigation, the vertical distribution of ventilation and perfusion was studied during anesthesia by means of radioactive isotopes to locate regions with shunt. The results were compared with the visible distribution of atelectasis on CT scans and with the distribution of ventilation-to-perfusion ($\dot{V}/\dot{Q}$) ratios as measured by the multiple inert gas elimination technique. Finally, $\dot{V}/\dot{Q}$ distributions by inert gas and isotope techniques were compared.

PATIENTS AND METHODS

Patients

Ten patients (3 women and 7 men, mean age 50 yr) scheduled for elective abdominal surgery were studied awake immediately before induction of and during general anesthesia. They were all of ordinary body configuration (Table 1). Five were smokers and five were nonsmokers. No one presented symptoms or signs of chronic bronchitis. Preoperative spirometry was within the normal range in all patients, although two smokers had low flows at the end of a forced expiration (20). The study was approved by the Ethical Committee of Huddinge University Hospital, and informed consent was obtained from each patient.

Anesthesia

The patients received no premedication. Atropine (0.25 mg iv) and fentanyl (0.1–0.2 mg iv) were given immediately before anesthesia. Anesthesia was induced by thiopentone sodium (200–450 mg iv), and succinylcholine (75–100 mg iv) was given before tracheal intubation. Muscular relaxation was continuously achieved with pancuronium bromide (total dose 11–19 mg iv). The patients were ventilated at a rate of 12 breaths/min with a Servo 900C ventilator (Siemens Elema) with zero end-expiratory pressure. Tidal volume was adjusted to result in an end-tidal carbon dioxide concentration of ~4%. Anesthesia was maintained with halothane, 0.6–1.3% inspired concentration, in a gas mixture of oxygen and nitrogen. The inspired oxygen fraction (0.40–0.43) was checked by mass spectrometry and kept constant during the measurements in each patient. Minute ventilation was monitored on a vortex meter (Bourns L5–75), and the airway pressures were monitored on the manometer of the ventilator.

Catheterization

A triple-lumen thermistor-tipped catheter (Swan-Ganz no. 7F, Edwards Laboratories) was introduced from a brachial vein to the pulmonary artery. A brachial arterial and two peripheral venous catheters were also inserted. One of the venous lines was used for infusion of inert gases and the other for injection of anesthetic drugs. Vascular pressures were measured relative to the atmospheric pressure, with the midthoracic level as reference. The pressures were averaged during the respiratory cycle. Cardiac output (mean of 3 measurements) was determined by standard thermodilution technique by use of 10-ml bolus injections of chilled (0–4°C) glucose solution (50 mg/ml). The thermal curve was analyzed by a cardiac output computer (model 9520A, Edwards Laboratories).

$\dot{V}/\dot{Q}$ Ratios

$\dot{V}/\dot{Q}$ distribution to lung regions with different $\dot{V}/\dot{Q}$ ratios was determined by a multiple inert gas elimination technique based on the infusion of a solution of six gases: sulfur hexafluoride, ethane, cyclopropane, enflurane, ether, and

Table 1. *Subject data*

Subject No.	Sex	Age, yr	Height, cm	Weight, kg	Cigarettes/ day	FVC, %pred	$FEV_{1.0}$, %pred	MEF_{25}, %pred
1	F	65	155	68	0	96	105	
2	F	62	162	77	0	117	130	94
3	F	32	174	72	20	112	102	95
4	M	36	183	80	0	107	100	136
5	M	58	179	85	5	86	95	140
6	M	60	182	74	20	111	90	44
7	M	49	180	67	0	110	97	81
8	M	56	185	88	0	135	118	55
9	M	20	178	75	20	117	107	93
10	M	49	178	88	10	87	87	48

FVC, forced vital capacity; $FEV_{1.0}$, forced expired volume in 1 s; MEF_{25}, expired flow at 25% vital capacity in percentage of predicted values (%pred) (20).

acetone (5, 33; for further technical details, see Ref. 32). Of the available information obtained from the $\dot{V}/\dot{Q}$ distribution, we present data on shunt ($\dot{Q}s$: perfusion of lung regions with $\dot{V}/\dot{Q} < 0.005$), "low $\dot{V}/\dot{Q}$ regions" ($\dot{Q}_{low}$: perfusion of lung regions with $0.005 < \dot{V}/\dot{Q} < 0.1$), "high $\dot{V}/\dot{Q}$ regions" ($\dot{V}_{high}$: ventilation of lung regions with $10 < \dot{V}/\dot{Q} < 100$), and dead space ($\dot{V}_D$: ventilation of lung regions with $\dot{V}/\dot{Q} > 100$) and the mean and the log standard deviation of the distribution of blood flow ($\dot{Q}_{mean}$ and log $\dot{Q}_{SD}$) and ventilation ($\dot{V}_{mean}$ and log $\dot{V}_{SD}$). Subdivisions of blood flow and of ventilation are presented as percentage of cardiac output and expired minute ventilation, respectively.

Blood Gas Analysis

Arterial and mixed venous blood samples were drawn for blood gas analysis, for which standard techniques were employed (ABL-2, Radiometer, Copenhagen, Denmark).

CT of the Chest

The development and the size of atelectasis were determined by X-ray CT scanning (Siemens Somatom 2) of the chest at two levels: at the top of the diaphragm (the position was determined from the frontal scout view in the awake state) and 5 cm cranially to the first level. During anesthesia, the same scan levels relative to the spine were used. The measurements were made during apnea at resting end-expiratory lung volume [functional residual capacity (FRC)]. Scan time was 5 s at 115 mA and 125 kV, and slice thickness was 8 mm. The total estimated dose equivalent from CT was 0.28 mSv. The transverse thoracic and atelectatic areas were measured by planimetry on the transverse CT scans. The thoracic area was defined as the area within the inner walls of the thoracic cage and includes the lungs and the mediastinal organs. The atelectatic area, defined as volume elements with attenuation values between −100 and 100 Hounsfield units (6), is presented as percentage of thoracic area. Maximal transverse and sagittal diameters were measured on the CT scans and refer to the inner margins of the thoracic cage.

Ventilation and Perfusion Scintigraphy of the Lungs

Two radionuclides with different gamma energies, ^{113m}In and ^{99m}Tc, were used for single-photon emission computerized tomography (SPECT). For ventilation scintigraphy, the patient inhaled an aerosol. The isotope was bound to diethylenetriamine pentaacetic acid (DTPA) dissolved in 3 ml of isotonic saline. The nebulizer (UltraVent, Mallinckrodt) produces an aerosol that, according to the manufacturer, has a median mass aerodynamic diameter of 0.5–0.6 μm with 98% of the particles <1.0 μm. For perfusion scintigraphy, the isotope was bound to macroaggregated human albumin (MAA), which was injected intravenously after the inhalation of aerosol. The total activity of the two isotopes was not allowed to exceed a dose equivalent of 1 mSv. We aimed at reaching an activity of ^{99m}Tc five times that of ^{113m}In, because In is partly seen in the Tc window. In the first five patients ^{113m}In-DTPA was inhaled (800 MBq in the nebulizer) and ^{99m}Tc-MAA was injected (37 MBq), which ensured a perfusion image of high statistical quality but a ventilation image of less quality. To optimize the statistical quality of the ventilation image without exceeding the permissible dose equivalent and yet maintain the activity ratio between the two isotopes, the next five patients inhaled ^{99m}Tc-DTPA (2,000 MBq in the nebulizer), and 37 MBq of ^{113m}In-MAA were injected. The mean counts collected in the first frontal projection (during 20 s) from the inhaled isotope were 41,000 (*patients 1–5*, ^{113m}In) and 258,000 counts (*patients 6–10*, ^{99m}Tc) and from the injected isotope 177,000 (*patients 1-5*, ^{99m}Tc) and 44,000 counts (*patients 6–10*, ^{113m}In). After the inhalation of aerosol was completed, the respiratory tubing, including the y piece, was replaced by noncontaminated tubing.

For tomography, a gamma camera (Maxi Camera 400T, General Electric) with a medium-energy collimator was rotated around the patient, who lay supine on the tomograph table with arms stretched cranially. Counts were collected in windows of 20% centered around the photo peaks at 140 and 392 keV (^{99m}Tc and ^{113m}In, respectively) simultaneously for both isotopes at 64 positions (360°). Acquisition time was 20 s at each position, and the data were stored in two 64 × 64 matrices by a computer (PDP/11, Digital Equipment). The first two positions were repeated at the end of the procedure to obtain an estimate of the effective half-life of the isotopes within the lung that was accounted for in the reconstruction of the ventilation and perfusion distributions (software: SPETS and Gamma-11, Digital Equipment). Attenuation correction for thoracic geometry was not used, inasmuch as no transmission source was available. The spatial resolution for this technique and equipment was ~11 mm.

Data Analysis

From the acquired data two sets of transverse scans covering all parts of both lungs were reconstructed: one set for ventilation and the other for lung perfusion. The scans were built up by volume elements (voxels) with the following dimensions: 0.58 × 0.58 × 1.16 cm (the largest dimension parallel to the axis of rotation, i.e., cranial-caudal direction).

Ventilated and perfused lung tissues were delineated according to the following procedure: the transverse diameter at midlung level of the two CT scans was measured. A background was subtracted from the corresponding SPECT scans (ventilation and perfusion scans treated separately) from all voxels to give transverse diameters of the ventilation and perfusion scans in agreement with the diameters of the CT scans (within the resolution of one voxel). If an exact agreement between the diameters was not found, we allowed the lungs on the SPECT scans to be slightly larger, inasmuch as these scans were obtained during tidal breathing and CT scans were obtained during apnea at FRC. The background, expressed as a percentage of the maximal activity of the two isotopes in any voxel (range 13–33%), was thus individually determined for each patient for both isotopes and was subtracted from all voxels in the tomographed volume (also within the lung). An impaction of aerosol in the carina and endotracheal tube was seen in most patients. This area was excluded. After the lungs were delineated, cardiac output and expired minute ventilation were divided by the total number

of counts of the corresponding isotope. Blood flow and ventilation to a single voxel were obtained by multiplying these ratios by the number of counts of the appropriate isotope within that voxel. The $\dot{V}/\dot{Q}$ ratio was calculated for each voxel, and the distribution of ventilation and blood flow against $\dot{V}/\dot{Q}$ ratios was plotted in a manner similar to the inert gas $\dot{V}/\dot{Q}$ data.

Vertical ventilation and perfusion profiles were constructed after normalization of lung dimensions.

Procedure and Technical Setup

The patients were catheterized in the awake state at the catheterization laboratory, after which they were moved to the X-ray department for measurements of hemodynamics and gas exchange during air breathing and for CT scans. They were then anesthetized as previously described. Another two transverse CT scans were obtained 15 min after induction of anesthesia. The patients were then moved to the isotope department during manual ventilation with 0.5–1% halothane in pure oxygen, where they were placed supine on the gamma camera tomograph table and connected to the ventilator. After another 20 min of anesthesia (inspired oxygen fraction 0.40–0.43), hemodynamics and gas exchange were measured, then inhalation of the aerosol tagged with isotope was started. The nebulizer (within a shielding container) was connected to the inspiratory tubing of the ventilator. The gas to the nebulizer (10 l/min) was obtained from the gas inlet to the ventilator after it passed the halothane vaporizer, permitting a stable anesthesia and an unchanged inspired oxygen fraction. The tidal volume given to the patient could not be directly controlled by the inspired volume setting of the ventilator because of the additional gas introduced to the respiratory tubing by the nebulizer. The ventilator tidal volume was set to result in the same inspiratory pause pressure as before the inhalation of aerosol, and the end-tidal carbon dioxide concentration did not change during the procedure. The exhaled gases passed a collection filter before they reached the expiratory flow sensor of the ventilator. After completion of aerosol inhalation, the intravenous isotope was slowly injected during mechanical ventilation, and the emission tomography was commenced. After conclusion of the measurements, all catheters but one venous line were removed and the patients were transported to the operation theater to undergo surgery. The study lasted ~2 h, including the awake measurements.

Statistics

Means ± SE were calculated. The significance of differences between the awake and the anesthetized paralyzed conditions was tested by Student's paired *t*-test (two-tailed). Linear regression analysis was performed to study the relationship between two variables.

RESULTS

Awake

Cardiac output, heart rate, and systemic and pulmonary vascular pressures were within the normal range during the awake state, whereas minute ventilation was rather high (4) (Table 2). Gas exchange was normal, with narrow perfusion and ventilation distributions, as assessed by the inert gas technique (Table 3). Shunt and perfusion of low $\dot{V}/\dot{Q}$ did not exceed 1 and 4%, respectively, in any patient. $\dot{V}_D$ (including apparatus dead space) comprised 30% of ventilation.

Table 2. *Circulatory and respiratory variables, arterial blood gases, and atelectasis*

Variable	Awake	Anesthesia
$\dot{Q}_T$, l/min	6.5 ± 0.3	5.7 ± 0.3†
HR, beats/min	70 ± 2	79 ± 3§
$\bar{P}a$, mmHg	14.3 ± 1.1	13.7 ± 1.1
$\bar{P}cv$, mmHg	7.7 ± 0.7	8.8 ± 0.9
$\bar{P}ba$, mmHg	104 ± 6.0	81 ± 5.7§
$\dot{V}_E$, l/min	9.1 ± 1.1	6.2 ± 0.3‡
Paw, cmH_2O		12.2 ± 1.1
Pa_{O_2}, Torr	95.0 ± 4.5	159.1 ± 10.1*
Pa_{CO_2}, Torr	36.1 ± 1.4	35.7 ± 0.9
Atelectatic *area 0*, %	0.0 ± 0.0	2.2 ± 0.7‡
Atelectatic *area 5*, %	0.0 ± 0.0	1.8 ± 0.7†

Values are means ± SE; $n = 10$. $\dot{Q}_T$, cardiac output; HR, heart rate; $\bar{P}a$, $\bar{P}cv$, and $\bar{P}ba$, mean pulmonary arterial, pulmonary capillary venous, and brachial arterial pressures, respectively; $\dot{V}_E$, expired minute ventilation; Paw, end-inspiratory airway pressure; Pa_{O_2} and Pa_{CO_2}, arterial P_{O_2} and P_{CO_2} ; *area 0* and *area 5*, transverse atelectatic area in percentage of transverse thoracic area at top of diaphragm and 5 cm cranially, respectively; *inspired O_2 fraction = 0.40–0.43. † $P < 0.05$; ‡ $P < 0.01$; § $P < 0.001$.

CT scanning displayed no lung abnormalities in any patient during the awake measurements.

Anesthesia With Muscle Paralysis and Mechanical Ventilation

Ventilation and hemodynamics. Minute ventilation was lower during anesthesia than in the awake condition (−31%; Table 2). Cardiac output decreased (−13%) and heart rate increased (13%). Mean pulmonary vascular pressures were unchanged, whereas mean systemic arterial pressure decreased (−21%).

Gas exchange. The distribution of perfusion, as assessed by the multiple inert gas elimination technique, was in most cases wider than during the awake state and centered around a lower mean value (Table 3; see Figs. 2 and 5). In all patients there was an increased

Table 3. *Distribution of perfusion and ventilation from multiple inert gas elimination technique in awake state and during anesthesia and from SPECT during anesthesia*

	Inert Gas Data		SPECT
Variable	Awake	Anesthesia	Anesthesia
$\dot{Q}_S$, %	0.2 ± 0.1	5.0 ± 1.3[a]	6.9 ± 1.9
$\dot{Q}_{low}$, %	1.2 ± 0.5	7.1 ± 1.8[a]	3.6 ± 0.8
$\dot{Q}_{mean}$	0.76 ± 0.10	0.51 ± 0.07[a]	0.94 ± 0.07[d]
log $\dot{Q}_{SD}$	0.67 ± 0.07	1.18 ± 0.12[a]	0.80 ± 0.04[c]
$\dot{V}_D$, %	30 ± 5.0	32 ± 3	5.3 ± 1.6[e]
$\dot{V}_{high}$, %	0.04 ± 0.04	0.0 ± 0.0	7.4 ± 1.8[d]
$\dot{V}_{mean}$	1.14 ± 0.16	1.01 ± 0.11	1.67 ± 0.13[e]
log $\dot{V}_{SD}$	0.54 ± 0.06	0.62 ± 0.05[b]	0.78 ± 0.04[c]

Values are means ± SE; $n = 10$. $\dot{Q}_S$ and $\dot{Q}_{low}$; shunt and perfusion of regions with $0.005 < \dot{V}/\dot{Q} < 0.1$, respectively, expressed as percentage of cardiac output; $\dot{Q}_{mean}$ and log $\dot{Q}_{SD}$, mean and log standard deviation of perfusion; $\dot{V}_D$ and $\dot{V}_{high}$, ventilation to regions with $\dot{V}/\dot{Q} > 100$ and $10 < \dot{V}/\dot{Q} < 100$, respectively, expressed as percentage of expired ventilation; $\dot{V}_{mean}$ and log $\dot{V}_{SD}$, mean and log standard deviation of ventilation. Significantly different from awake: [a] $P < 0.01$; [b] $P < 0.001$. Significantly different from inert gas data during anesthesia: [c] $P < 0.05$; [d] $P < 0.01$; [e] $P < 0.001$.

retention of the least soluble gases, which appeared as shunt and/or perfusion of low $\dot{V}/\dot{Q}$ regions. Shunt ranged from 0.4 to 12.2% and perfusion to low $\dot{V}/\dot{Q}$ regions from 0 to 18.0%. The distribution of the ventilation was confined to one main mode centered at the same mean value as during the awake situation. $\dot{V}_D$ was unaltered. Arterial oxygen tension was 125–202 Torr. Mean arterial carbon dioxide tension was unchanged (range 32–40 Torr) compared with the awake measurement.

CT and SPECT. Atelectasis appeared in dependent lung regions in nine patients. The atelectasis comprised 0.6–7.2% of the thoracic area, and the mean area was slightly larger in the caudal than in the cranial scan (Table 2, Figs. 1 and 2).

The subtraction criteria used for delineating the lung on the SPECT scan resulted in an overestimation of sagittal (ventral-dorsal) diameters compared with the corresponding CT scans by 0.3 ± 0.4 cm (CT: 18.0 ± 0.5 cm; $P > 0.05$) and 0.7 ± 0.5 cm (CT: 17.0 ± 0.4 cm; $P < 0.01$) at the caudal and cranial scan level, respectively. Lung volume estimated by SPECT was 2,590 ± 181 ml (range 1,600–3,500 ml).

After normalization of lung height, mean curves of the vertical ventilation and perfusion were calculated. After an initial increase down the topmost region, ventilation decreased further down the lung. Perfusion increased downward, except for the most dependent part, where it decreased (Fig. 3).

A more detailed analysis of the distributions was also undertaken by dividing the lung into four segments from the apex to the base (Fig. 4). Such an analysis showed that the inequality of ventilation and perfusion in the vertical direction increased from the apex to the base of the lung. Ventilation of poorly perfused regions was mainly found at the ventral aspects of the two basal segments of the lung. Shunt was seen in all four segments (Fig. 4) and was as large as 17% in the basal lung segment. In the other segments, it averaged 5–6%. Shunt was spread over a wider vertical distance in the apical lung segments than in the other segments, where shunt was mainly confined to dependent lung regions. Perfusion of poorly ventilated regions was generally small as measured by the isotope technique (Table 3). It was mainly located in dependent parts just above regions with shunted blood flow.

$\dot{V}/\dot{Q}$ distribution. Higher $\dot{V}_{mean}$ and $\dot{Q}_{mean}$ values were seen with the isotope technique than with the inert gas technique ($P < 0.01$ and $P < 0.001$, respectively). Moreover, with the isotope technique, the log $\dot{V}_{SD}$ was higher ($P < 0.05$) and the log $\dot{Q}_{SD}$ was lower ($P < 0.05$) than with the inert gas technique (Table 3). There was no significant difference between the mean values of shunt with use of isotope and inert gas techniques, respectively ($\dot{Q}s_{iso}$, $\dot{Q}s_{gas}$), and a correlation was found according to the following equation: $\dot{Q}s_{iso} = 0.29 + 1.26 \times \dot{Q}s_{gas}$ ($n = 10$, $r = 0.78$, $P < 0.01$). Perfusion to poorly ventilated regions tended to be lower for the isotope than for the inert gas technique ($P = 0.08$). The isotope technique showed regions with high $\dot{V}/\dot{Q}$ ($10 < \dot{V}/\dot{Q} < 100$), but the inert gas technique did not ($P < 0.01$; Table 3). The isotope technique detected only a small amount of dead space (defined as voxels with $\dot{V}/\dot{Q} > 100$), 5% vs. 32% with the inert gas method ($P < 0.001$). Individual $\dot{V}/\dot{Q}$ distributions are shown in Fig. 5.

Shunt vs. atelectasis. Shunt measured by the inert gas technique correlated with the size of atelectasis (x) according to the following regression equation: $\dot{Q}s_{gas} = 1.03 + 1.78 \times x$ ($n = 10$, $r = 0.91$, $P < 0.001$). Also, shunt measured by the isotope technique correlated with the size of atelectasis: $\dot{Q}s_{iso} = 2.00 + 2.18 \times x$ ($n = 10$, $r = 0.76$, $P < 0.01$).

CT scans and the corresponding SPECT scans from five patients are shown in Figs. 1, 2, and 6. On the SPECT scan, the area in which shunt was found has been indicated, and it closely agrees with the location of atelectasis. Figures 1 and 2 show examples of large and small atelectasis with accompanying large and small shunts (*patients 10* and *3*). In *patient 6*, narrow atelectatic regions bridged over a rim of aerated alveoli in the bottommost part of the lung. The corresponding SPECT scan disclosed a horizontal zone of shunt resting on a perfused and ventilated region (Fig. 6, *A* and *B*). In *patient 5*, the CT showed a trabeculated atelectasis similar to a honeycomb pattern. The SPECT scan showed a large mottled shunt area corresponding to the atelectatic region (Fig. 6, *C* and *D*). *Patient 4* had only minor atelectasis in dependent parts of both lungs, as seen on the CT scan. Shunt in this patient was found as a narrow rim in the bottom of the lungs (Fig. 6, *E* and *F*). However, despite individual similarities, shunt tended to extend higher up in the vertical direction than in the atelectatic region. This may in part have been due to the finding of a shunt along the mediastinal lung border in three of five patients who received ^{113m}In-MAA for blood flow measurements (but in none with ^{99m}Tc-MAA; cf. Fig. 1).

This finding was unexpected and forced us to perform model experiments with two glass bottles filled with saline to which two isotopes (^{113m}In and ^{99m}Tc) were added. The bottles were 10 cm in diameter and 5 cm apart, simulating the lungs and mediastinum in a transverse projection. In the transverse SPECT scans there was a rim of pure ^{113m}In activity along the mediastinal aspects of the bottles but not elsewhere (Fig. 7). Thus the "mediastinal" shunt may be an artifact caused by reconstruction errors.

DISCUSSION

Atelectasis in dependent parts of the lung is a regular finding during anesthesia with muscle paralysis and mechanical ventilation, appearing shortly after induction of anesthesia and before surgery (2, 27). A right-to-left shunt of blood has been found to correlate with the size of atelectasis (30). We have shown that the shunt is located in the dependent atelectatic lung regions. In addition, a marked inhomogeneity of the vertical ventilation and perfusion distributions was found.

Methods

Before we discuss the results, several methodological aspects should be considered. Three major methods have been used: CT, the multiple inert gas elimination

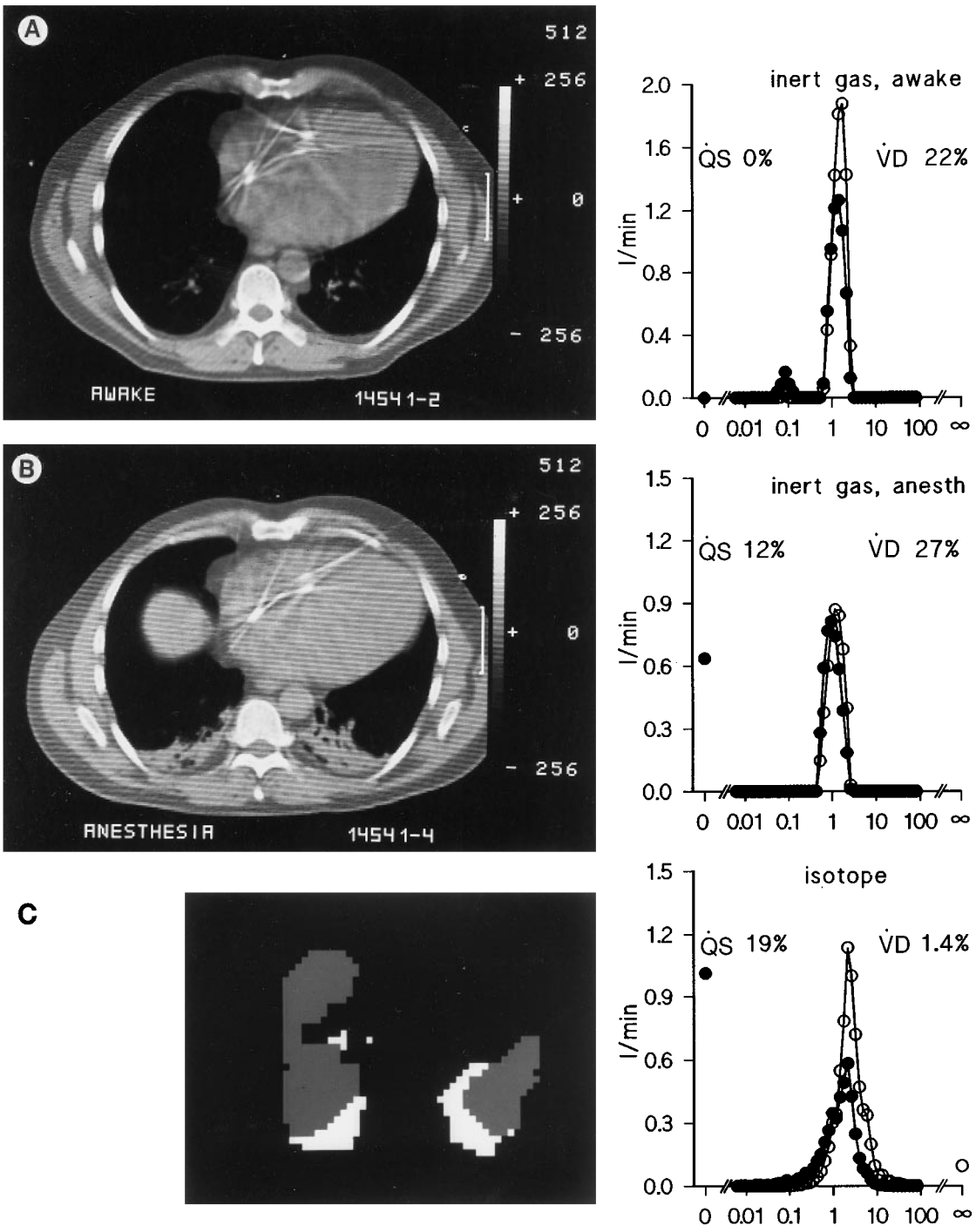

Fig. 1. Computerized tomography (CT) scans and inert gas ventilation-perfusion ($\dot{V}/\dot{Q}$) distributions of ventilation and perfusion in *patient 10* in awake state (*A*) and during anesthesia-paralysis (*B*), as well as corresponding transverse slice and $\dot{V}/\dot{Q}$ distributions reconstructed from single-photon emission CT (SPECT) during anesthesia (*C*). *x*-Axis, $\dot{V}/\dot{Q}$ ratios; *y*-axis, ventilation (○) and perfusion (●). Note absence of lung densities and normal $\dot{V}/\dot{Q}$ distribution in awake state and appearance of large densities (atelectasis) in dependent lung regions during anesthesia. Concomitantly, a large shunt was measured with inert gas and isotope techniques. Voxels with $\dot{V}/\dot{Q}$ ratio <0.005 (shunt) have been colored white on transverse slice from SPECT. Note location of shunt in dependent lung regions. $\dot{Q}_S$, shunt as percentage of cardiac output ($\dot{V}/\dot{Q} < 0.005$; ● at zero on *x*-axis); $\dot{V}_D$, dead space ventilation as percentage of expired minute ventilation ($\dot{V}/\dot{Q} > 100$; ○ in *C* at infinity; in *A* and *B*, $\dot{V}_D$ is out of range of *y*-axis).

technique, and SPECT. By CT, two scans of the thorax, 5 cm apart, were obtained. Morphological changes can be visualized with a high spatial resolution within these scans, but there is no information about other parts of the lung, and little information about function is provided. The multiple inert gas elimination technique measures the functional properties of the lung with regard to the distribution of ventilation and perfusion relative to $\dot{V}/\dot{Q}$ ratios (5, 33). The technique has the ability to separate regions with low $\dot{V}/\dot{Q}$ ratios from

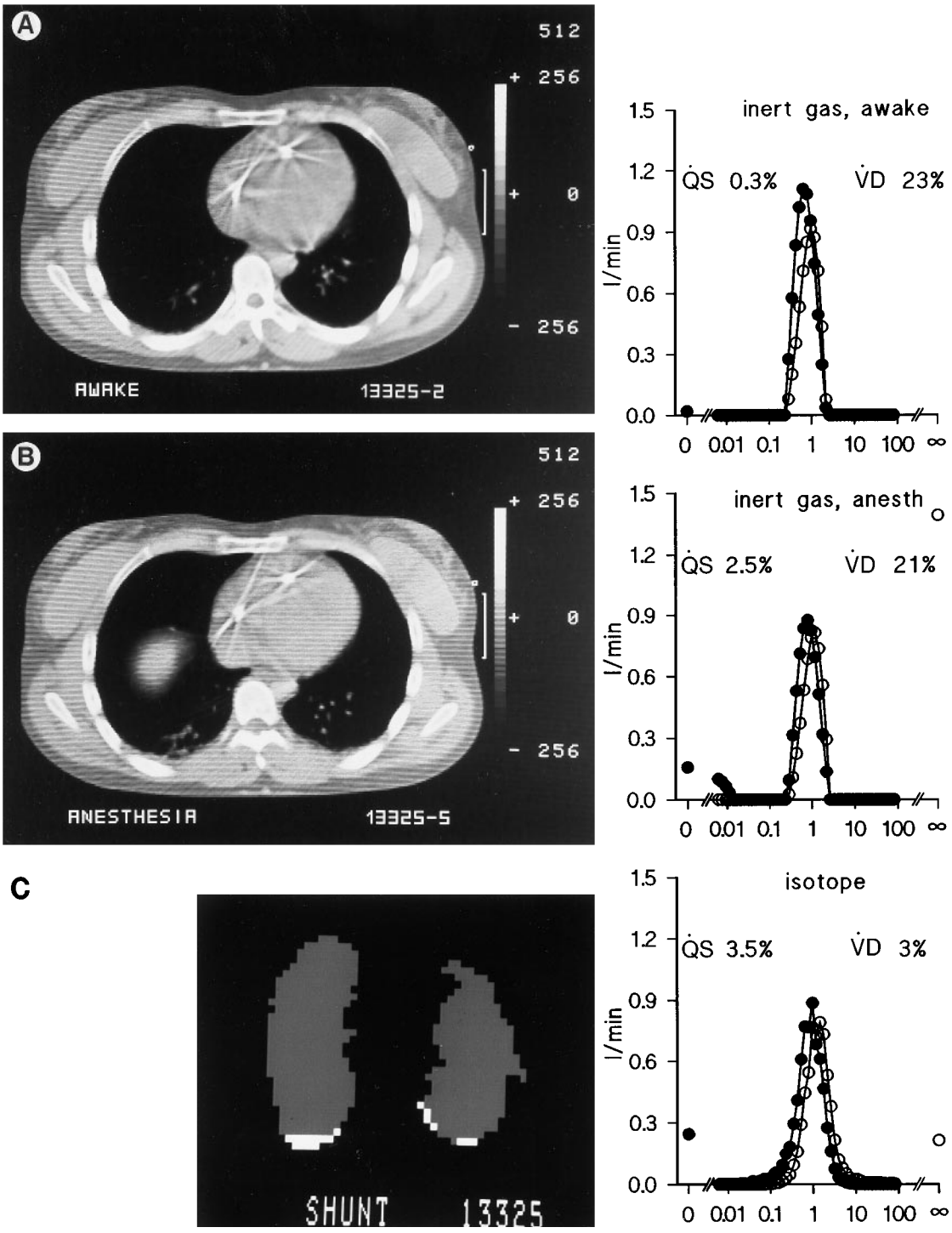

Fig. 2. CT scans and inert gas $\dot{V}/\dot{Q}$ distributions of ventilation and perfusion in *patient 3* in awake state (*A*) and during anesthesia-paralysis (*B*), as well as corresponding transverse slice and $\dot{V}/\dot{Q}$ distributions reconstructed from SPECT during anesthesia (*C*). *x*-Axis, $\dot{V}/\dot{Q}$ ratios; *y*-axis, ventilation (○) and perfusion (●). Note minor atelectatic area on CT during anesthesia and appearance of a small shunt located in dependent lung regions on transverse slice from SPECT (white regions). $\dot{Q}S$, shunt as percentage of cardiac output ($\dot{V}/\dot{Q} < 0.005$; ● at zero on *x*-axis); $\dot{V}D$, dead space ventilation as percentage of expired minute ventilation ($\dot{V}/\dot{Q} > 100$; ○ in *B* and *C* at infinity; in *A*, $\dot{V}D$ is out of range of *y*-axis).

shunt and also well-ventilated regions with only minor perfusion from dead space. However, it renders no information about the spatial distribution of ventilation and perfusion within the lung. Scintigraphy provides a localization of function within a tissue, as measured by the distribution of an isotope, and in combination with CT this can be performed in three dimensions. SPECT is, however, considered to have less spatial resolution than CT. The distribution of injected isotope-labeled MAA has been shown to accurately display the distribution of blood flow by the time of entrapment of the particles in the capillaries (31).

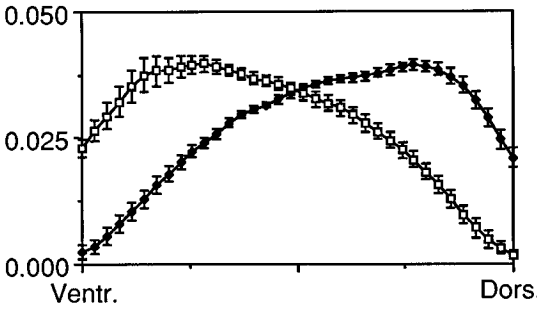

Fig. 3. Vertical distribution of mean fractional ventilation (□) and perfusion (●) in supine anesthetized patients. Values are means ± SE; $n = 10$. Lung dimensions have been normalized. Ventr, ventral; Dors, dorsal.

Ventilation scintigraphy with isotope-labeled aerosol has been used for 30 years (19, 29). It relies on the assumption that the aerosol will be distributed within the lungs in relation to ventilation. This assumption seems to be approximately valid for particles with an aerodynamic diameter <1 μm (12, 18, 25). The nebulizer used in the present investigation has been reported to produce an aerosol that results in little impaction in central airways and a distribution within the lung comparable to that of the gas ^{81m}Kr (34). Animal experiments indicate that small-sized aerosols are deposited mainly in respiratory units also during mechanical ventilation (25). We found some impaction on the carina and the endotracheal tube, but over the lung the distribution of the inhaled isotope was smooth, with no "hot spots" in any patient. Thus impaction seemed to be no major problem. The retention of aerosols has been shown to decrease and the clearance to increase with increasing lung volume (3, 25), and because of differences in alveolar expansion (15), ventilation may be underestimated in nondependent compared with dependent parts of the lung. Also, alveoli that are expanded mainly by dead space gas during tidal breathing appear well ventilated because of the abundance of aerosol in dead space, whereas their contribution to gas exchange may be minimal, as measured by the inert gas technique. These methodological difficulties should, however, not invalidate the aerosol technique in detecting shunt.

The range of background subtraction values used for delineating the lungs on the SPECT scans embraces the value of 20%, which resulted in a good transverse area estimation of a lung phantom (17). We used individual subtraction values based on measured transverse diameters, which resulted in a good correspondence between ventral-dorsal lung diameters measured by SPECT and CT. Mean lung volume was estimated at 2.6 liters, including air, tissue, and blood volume. The weight of the lungs is 900–1,000 g (14). Reducing blood volume by 100–200 ml [as caused by anesthesia and mechanical ventilation (10)] and adding 100 ml for the volume of extrapulmonary airways, the calculated mean gas volume (FRC) approximates 2.0 liters. This is close to the anticipated mean FRC (2.1 liters) of our patients during anesthesia in the supine position by use of the summary equation of Rehder and Marsh (23).

Atelectasis and Shunt

Atelectasis was found in 9 of 10 patients in this study, which compares with our previous findings during anesthesia with muscle paralysis (2, 8). Shunt was also demonstrated in the same nine patients, and there was a correlation, and similar mean values, between inert gas shunt and isotope shunt. Shunt, demonstrated by either technique, correlated with the atelectatic area, and by SPECT the shunt could be located in the dependent lung regions. There was a fair individual correspondence between atelectasis on CT scans and the distribution of shunt on SPECT scans. The mediastinal shunt in a few patients was most likely explained by reconstruction errors of the SPECT scans. Thus the only clear location of shunt was the dependent (dorsal) lung regions. Shunt was distributed among all four segments from apex to base. Although no CT scans were made at the level of the two apical segments, previous studies indicate that in approximately one-half of the patients atelectasis can be found 10 cm cranial to the diaphragm (2), corresponding to the lower part of the most apical segment in the present study.

Distribution of Ventilation and Perfusion

The finding of a decrease in ventilation down the lung from frontal to dorsal (vertical direction) confirms previous findings in anesthetized paralyzed humans (1, 13, 16, 22, 24). However, in previous studies no detailed analysis of ventilation distribution was possible. They have been limited to measurements of distribution between the two lungs in the lateral position or to a few vertical levels in the supine position. In this study, we noted a reduced ventilation in the topmost region, which might be related to well-expanded alveoli located on the upper flatter part of their pressure-volume curve (cf. Ref. 15). There is also the possibility of a compensatory reduction of ventilation because of reduced blood flow, as demonstrated by Severinghaus et al. (26) and attributed to hypocapnic bronchoconstriction. Finally, by addition of perfusion data by means of the macroaggregate technique, a zone of no ventilation in the most dependent part of the lung could be detected. This would not have been possible by intravenous injection of Xe, as has been used in earlier studies, because its demonstration of lung blood flow requires that it diffuses to patent alveoli. A nonventilated zone because of lung collapse (atelectasis) would thus not have been detected.

The general feature of an increase in perfusion down the lung is similar to that reported earlier in anesthetized paralyzed humans (13, 16). However, a much more detailed analysis was made possible by the presently used technique. Thus the vertical gradient of perfusion, from top to bottom, displayed an initially steep increase followed by a region with less increase (compatible with zones 2 and 3) and, finally, a decrease of perfusion in the lowermost region of the lung (zone 4; Figs. 3 and 4) (14). The findings are similar in detail to those obtained in anesthetized dogs and have been attributed to gravitational forces, although nongravita-

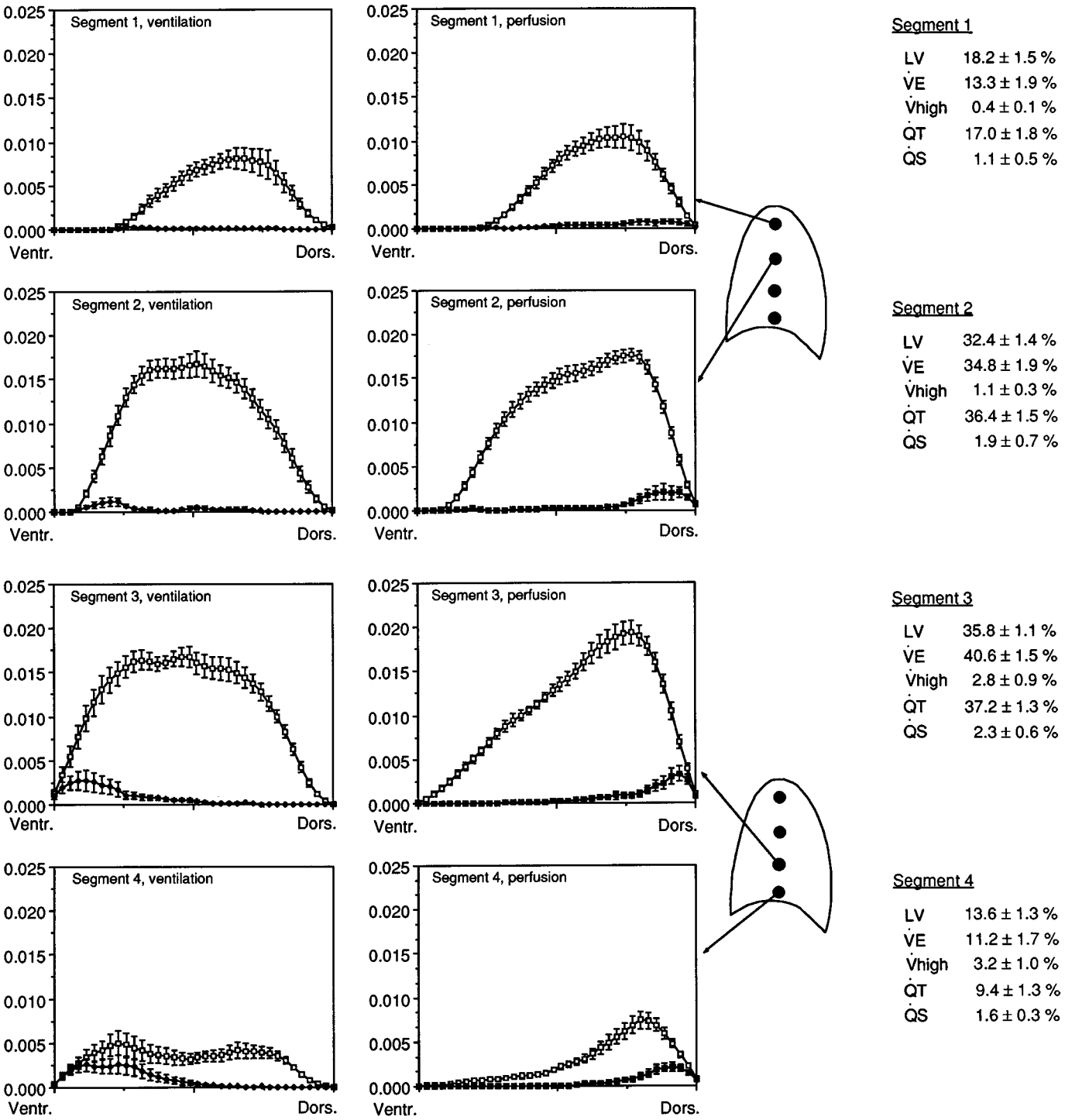

Fig. 4. Vertical (ventral-dorsal) distributions of mean fractional ventilation and perfusion (and subdivisions thereof) in 4 segments of lung from apex (*segment 1*) to base (*segment 4*) calculated from SPECT in anesthetized supine patients. Values are means ± SE; $n = 10$. *Left*: distribution of fractional expired ventilation (□) and ventilation of high $\dot{V}/\dot{Q}$ regions (◆); *right*: distribution of fractional perfusion (□) and shunt (◆). *x*-Axis, normalized ventral-dorsal lung height in arbitrary units. Data for each lung segment are shown in column at *right*. LV, fractional lung volume; $\dot{V}_E$, fractional expired ventilation; $\dot{V}_{high}$, ventilation of high $\dot{V}/\dot{Q}$ regions ($10 < \dot{V}/\dot{Q} < 100$) as fraction of $\dot{V}_E$; $\dot{Q}_T$, fractional lung blood flow; $\dot{Q}_S$, shunt ($\dot{V}/\dot{Q} < 0.005$) as fraction of $\dot{Q}_T$.

tional mechanisms also have been proposed (7, 9, 11, 21). In the most caudal segment, but not elsewhere, there were even findings compatible with an uppermost nonperfused zone 1. With the knowledge that mean pulmonary arterial pressure averaged 18.5 cmH_2O (13.7 mmHg) related to midthorax, sagittal diameter was 18 cm, and end-inspiratory airway and, presumably, alveolar pressure was 12.2 cmH_2O (Tables 2 and 4), it can be assumed that alveolar pressure exceeded pulmonary vascular pressure during part but not all of

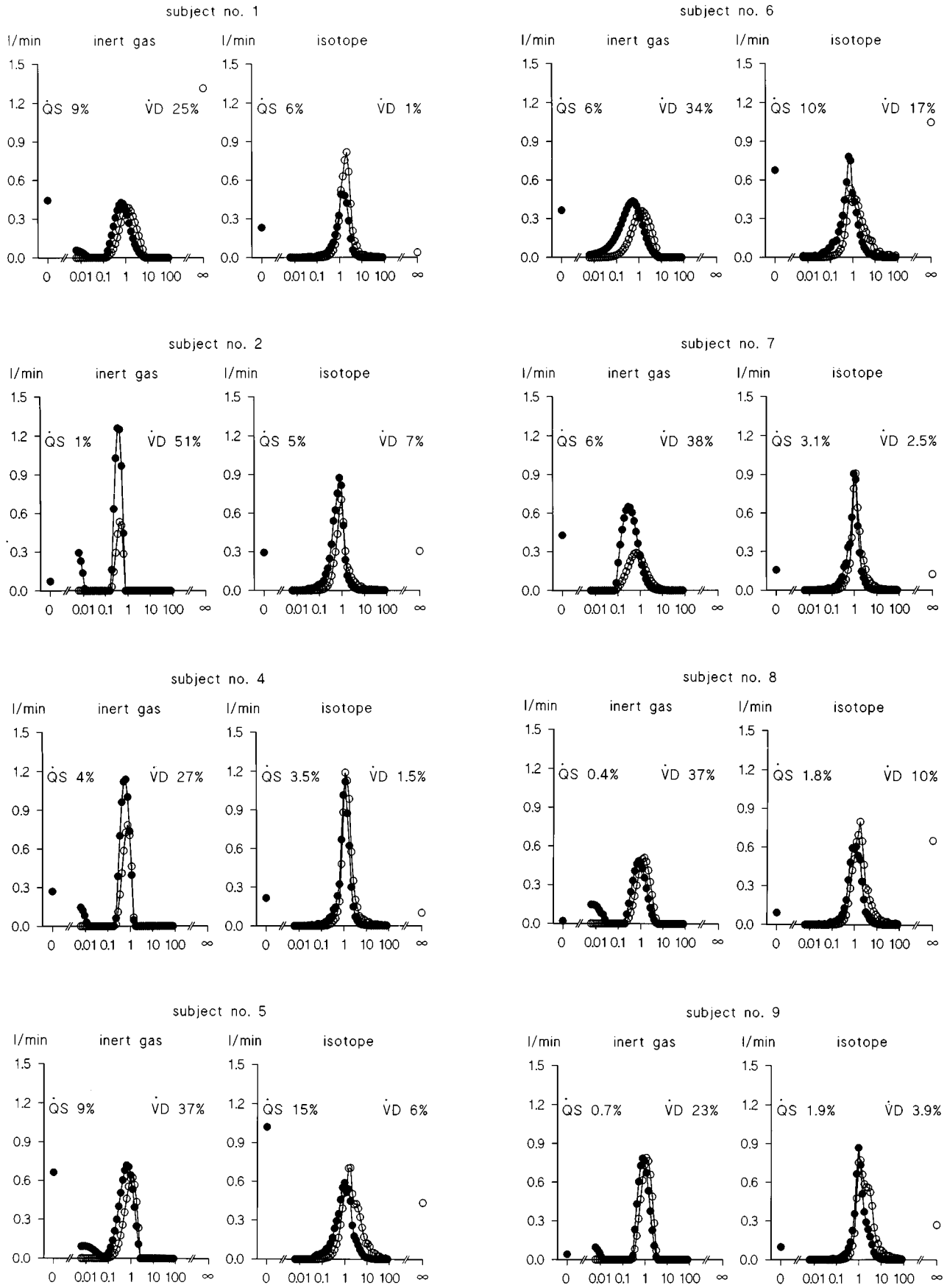

Fig. 5. Individual V̇/Q̇ distributions during anesthesia. *Left*: inert gas data; *right*: isotope data. *x*-Axis, V̇/Q̇ ratios; *y*-axis, ventilation (○) and perfusion (●). Note similarity between V̇/Q̇ distributions with the 2 techniques in most patients, except for dead space values.

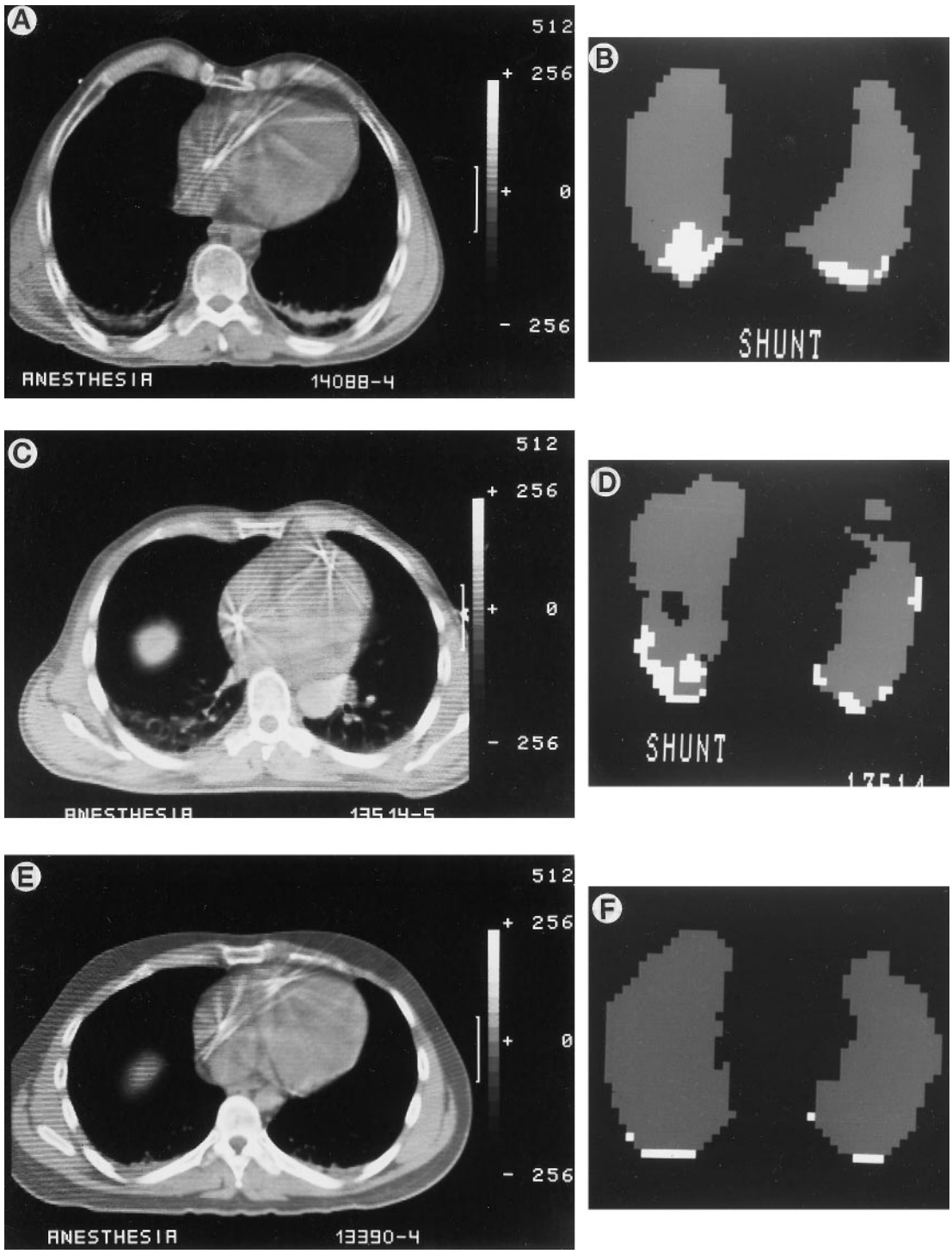

Fig. 6. CT (*A, patient 6; C, patient 5; E, patient 4*) and SPECT scans (*B, patient 6; D, patient 5; F, patient 4*) during anesthesia. Note close correspondence between distributions of atelectasis and of shunt (white voxels).

the respiratory cycle in nondependent lung regions. A similar discrepancy with a zero blood flow at a vertical level below the point where mean pulmonary arterial pressure is less than alveolar pressure has been reported by Reed and Wood (21).

No analysis of nongravitational distribution of ventilation and blood flow has been made in the present study.

$\dot{V}/\dot{Q}$ Ratios

The $\dot{V}/\dot{Q}$ distribution, assessed by the inert gas method, was similar to that in previous studies in subjects of similar age, both awake and during anesthesia (8, 30). Thus an increase in log $\dot{Q}_{SD}$ and a similar but smaller increase in log $\dot{V}_{SD}$ were seen during anesthesia, indicating an increased dispersion of $\dot{V}/\dot{Q}$ ratios. This

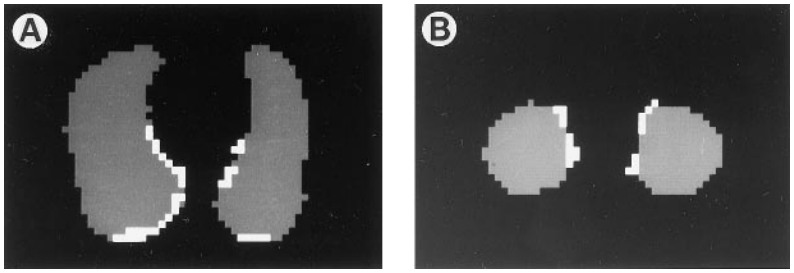

Fig. 7. Distribution of shunt (white voxels) on SPECT scan of *patient 7* (*A*) and a phantom experiment on 2 glass bottles filled with ^{113m}In and ^{99m}Tc dissolved in saline (*B*). Note rim of shunt along mediastinal border in patient in addition to shunt in dependent lung regions; also note that a similar rim appeared in phantom experiment, suggesting a reconstruction error in mediastinal area.

was also seen as an increased amount of perfusion of poorly ventilated lung regions ($\dot{Q}_{low}$, $\dot{V}/\dot{Q} < 0.1$).

Although the gross appearance of the $\dot{V}/\dot{Q}$ distributions by the isotope technique was similar to that of the inert gas method (Figs. 1, 2, and 5), significant differences in several indexes were also noted (Table 3). Thus the $\dot{V}/\dot{Q}$ distribution was shifted to the right, as evidenced by higher mean values of ventilation and blood flow; there was no $\dot{Q}_{low}$, but the presence of regions with ventilation in excess of perfusion ($\dot{V}_{high}$, $\dot{V}/\dot{Q} > 10$) and, finally, dead space was minor with the isotope technique. When the two methods are compared, it should be remembered that the inert gas method is based on gas dilution principles, whereas the used isotope technique is based on the deposition of particles in the alveoli and pulmonary vessels. The inert gas method enables the analysis of the distribution of alveolar ventilation relative to $\dot{V}/\dot{Q}$ ratios and can handle the V_D, whether of airways or of alveoli, separately. The isotope technique will depend on its resolution in detecting dead space. Thus any airway or alveolar region that is smaller than the voxel ($0.58 \times 0.58 \times 1.16$ cm) will not show up as dead space but will be included in the distribution of $\dot{V}/\dot{Q}$ ratios. This will explain the large difference in calculated dead space by the two methods (32 and 5%, respectively). This also explains the rightward shift of the $\dot{V}/\dot{Q}$ distributions. Moreover, it also explains the lower log $\dot{Q}_{SD}$ and higher log $\dot{V}_{SD}$ with the isotope technique, because a rightward shift of the distribution curves reduces the amount of $\dot{Q}_{low}$ and increases the amount of $\dot{V}_{high}$. Recalculation of the isotope distribution mean values after subtraction of the measured inert gas dead space shifted $\dot{V}/\dot{Q}$ distributions toward the left ($\dot{V}_{mean}$: 1.13; $\dot{Q}_{mean}$: 0.64) so that they came closer to the inert gas data (1.01 and 0.51, respectively).

Conclusions

This study has described the relationship between atelectasis and shunt in dependent lung regions during anesthesia and mechanical ventilation in supine patients. A preferential distribution of ventilation toward ventral lung regions and no or only minor perfusion of nondependent regions were seen. The $\dot{V}/\dot{Q}$ distribution calculated from isotope data was similar to that obtained by multiple inert gas elimination.

This study was supported by Swedish Medical Research Council Grant 5315 and grants from the Karolinska Institute and the Swedish Heart-Lung Fund.

Address for reprint requests: L. Tokics, Dept. of Anesthesiology, Huddinge University Hospital, S-141 86 Huddinge, Sweden.

Received 5 December 1995; accepted in final form 2 April 1996.

REFERENCES

1. **Bindslev, L., J. Santesson, and G. Hedenstierna.** Distribution of inspired gas to each lung in anaesthetized human subjects. *Acta Anaesthesiol. Scand.* 25: 297–302, 1981.
2. **Brismar, B., G. Hedenstierna, H. Lundquist, Å. Strandberg, L. Svensson, and L. Tokics.** Pulmonary densities during anesthesia with muscular relaxation—a proposal of atelectasis. *Anesthesiology* 62: 422–428, 1985.
3. **Davies, C. N., J. Heyder, and M. C. Summa Ramu.** Breathing of half-micron aerosols. I. Experimental. *J. Appl. Physiol.* 32: 591–600, 1972.
4. **Ekelund, L. G., and A. Holmgren.** Central hemodynamics during exercise. *Circ. Res.* 20, *Suppl.* 1: 33–43, 1967.
5. **Evans, J. W., and P. D. Wagner.** Limits on $\dot{V}_A/\dot{Q}$ distributions from analysis of experimental inert gas elimination. *J. Appl. Physiol.* 42: 889–898, 1977.
6. **Gattinoni, L. A. Pesenti, M. Bombino, S. Baglioni, M. Rivolta, F. Rossi, G. Rossi, R. Fumagalli, R. Marcolin, D. Mascheroni, and A. Torresin.** Relationships between lung computed tomographic density, gas exchange, and PEEP in acute respiratory failure. *Anesthesiology* 69: 824–832, 1988.
7. **Glenny, R. W., W. J. E. Lamm, R. K. Albert, and H. T. Robertson.** Gravity is a minor determinant of pulmonary blood flow distribution. *J. Appl. Physiol.* 71: 620–629, 1991.
8. **Gunnarsson, L., L. Tokics, H. Gustavsson, and G. Hedenstierna.** Influence of age on atelectasis formation and gas exchange impairment during general anaesthesia. *Br. J. Anaesth.* 66: 423–432, 1991.
9. **Hakim, T. S., G. W. Dean, and R. Lisbona.** Effect of body posture on spatial distribution of pulmonary blood flow. *J. Appl. Physiol.* 64: 1160–1170, 1988.
10. **Hedenstierna, G., Å. Strandberg, B. Brismar, H. Lundquist, L. Svensson, and L. Tokics.** Functional residual capacity, thoracoabdominal dimensions, and central blood volume during anesthesia with muscle paralysis and mechanical ventilation. *Anesthesiology* 62: 247–254, 1985.
11. **Hedenstierna, G., F. White, and P. D. Wagner.** Spatial distribution of pulmonary blood flow in the dog during positive end-expiratory pressure ventilation. *J. Appl. Physiol.* 47: 938–946, 1979.
12. **Heyder, J., and C. N. Davies.** The breathing of half-micron aerosols. III. Dispersion of particles in the respiratory tract. *J. Aerosol Sci.* 2: 437–452, 1971.
13. **Hulands, G. H., R. Greene, L. D. Iliff, and J. F. Nunn.** Influence of anaesthesia on the regional distribution of perfusion and ventilation in the lung. *Clin. Sci. Lond.* 38: 451–460, 1970.
14. **Commission on Radiological Protection (IRCP).** *Report of the Task Group on Reference Man.* New York: Pergamon, 1975, p. 158–160.
15. **Kaneko, K., J. Milic-Emili, M. B. Dolovich, A. Dawson, and D. V. Bates.** Regional distribution of ventilation and perfusion as a function of body position. *J. Appl. Physiol.* 21: 767–777, 1966.
16. **Landmark, S. J., T. J. Knopp, K. Rehder, and A. D Sessler.** Regional pulmonary perfusion and $\dot{V}/\dot{Q}$ in awake and anesthetized-paralyzed man. *J. Appl. Physiol.* 43: 993–1000, 1977.

17. **Macey, D. J., and R. Marshall.** In: *Computed Emission Tomography*, edited by P. J. Ell and B. L. Holman. Oxford, UK: Oxford University Press, 1982, p. 495–520.
18. **Morrow, P. E.** Task group on lung dynamics, deposition and retention models for internal dosimetry of the human respiratory tract. *Health Phys.* 12: 173–207, 1966.
19. **Pircher, F. J., J. R. Temple, W. J. Kirsch, and R. J. Reeves.** Distribution of pulmonary ventilation determined by radioisotope scanning. *Am. J. Roentgenol.* 94: 807–814, 1965.
20. **Quanjer, P. H** Standardized lung function testing. *Bull. Eur. Physiopathol. Respir.* 19, *Suppl.* 5: 7–10, 1983.
21. **Reed, J. H., and E. H. Wood.** Effect of body position on vertical distribution of pulmonary blood flow. *J. Appl. Physiol.* 28: 303–311, 1970.
22. **Rehder, K., D. J. Hatch, A. Sessler, and W. S. Fowler.** The function of each lung of anesthetized and paralyzed man during mechanical ventilation. *Anesthesiology* 37: 16–26, 1972.
23. **Rehder, K., and H. M. Marsh.** Respiratory mechanics during anesthesia and mechanical ventilation. In: *Handbook of Physiology. The Respiratory System. Mechanics of Breathing*. Bethesda, MD: Am. Physiol. Soc., 1986, sect. 3, vol. III, pt. 2, chapt. 43, p. 737–752.
24. **Rehder, K., A. D. Sessler, and J. R. Rodarte.** Regional intrapulmonary gas distribution in awake and anesthetized-paralyzed man. *J. Appl. Physiol.* 42: 391–402, 1977.
25. **Rizk, N. W., J. M. Luce, J. M. Hoeffel, D. C. Price, and J. F. Murray.** Site of deposition and factors affecting clearance of aerosolized solute from canine lungs. *J. Appl. Physiol.* 56: 723–729, 1984.
26. **Severinghaus, J. W., E. W. Swenson, T. N. Finley, N. T. Lategola, and J. Williams.** Unilateral hypoventilation produced in dogs by occluding one pulmonary artery. *J. Appl. Physiol.* 16: 53–60, 1961.
27. **Strandberg, Å., B. Brismar, G. Hedenstierna, H. Lundquist, and L. Tokics.** Atelectasis during anaesthesia and in the postoperative period. *Acta Anaesthesiol. Scand.* 30: 154–158, 1986.
28. **Strandberg, Å., G. Hedenstierna, L. Tokics, H. Lundquist, and B. Brismar.** Densities in dependent lung regions during anaesthesia: atelectasis or fluid accumulation? *Acta Anaesthesiol. Scand.* 30: 256–259, 1986.
29. **Taplin, G. V., and N. D. Poe.** A dual lung scanning technique for evaluation of pulmonary function. *Radiology* 85: 365–368, 1965.
30. **Tokics, L., G. Hedenstierna, Å. Strandberg, B. Brismar, and H. Lundquist.** Lung collapse and gas exchange during general anesthesia: effects of spontaneous breathing, muscle paralysis, and positive end-expiratory pressure. *Anesthesiology* 66: 157–167, 1987.
31. **Tow, D. E., H. N. Wagner, Jr., V. Lopez-Majano, E. M. Smith, and T. Migita.** Validity of measuring regional pulmonary arterial blood flow with macroaggregates of human serum albumin. *Am. J. Roentgenol.* 96: 664–676, 1966.
32. **Wagner, P. D., P. F. Naumann, and R. B. Laravuso.** Simultaneous measurement of eight foreign gases in blood gas chromatography. *J. Appl. Physiol.* 36: 600–605, 1974.
33. **Wagner, P. D., H. A. Salzman, and J. B. West.** Measurement of continuous distributions of ventilation-perfusion ratios: theory. *J. Appl. Physiol.* 36: 588–599, 1974.
34. **Wollmer, P., L. Eriksson, and A.-C. Andersson.** Clinical assessment of a commercial delivery system for aerosol ventilation scanning by comparison with krypton-81m. *J. Nucl. Med. Technol.* 13: 63–67, 1985.